RESEARCH ARTICLE

ADMM-Based Multi-Objective Control Scheme for Mitigating the Impact of High Penetration DER Integration in the Modern Distribution Systems

SADAF RAHIMI FAR, (Graduate Student Member, IEEE),
ALI MOEINI, (Senior Member, IEEE), **AMBRISH CHANDRA**, (Fellow, IEEE),
AND INNOCENT KAMWA, (Fellow, IEEE)

École de Technologie Supérieure, Université du Québec, Montréal, QC H3C 1K3, Canada
Hydro-Québec Research Institute, Montréal, QC J3X 1S1, Canada
Department of Electrical Engineering and Computer Engineering, Faculty of Science and Engineering, Laval University, Québec City, QC G1V 0A6, Canada

Corresponding author: Sadaf Rahimi Far (sadaf.rahimi-far.1@ens.etsmtl.ca)

ABSTRACT The high penetration of renewable energy sources in modern distribution networks poses challenges for grid voltage regulation. In this study, a multi-agent distributed voltage control strategy based on the proximal Jacobian alternating direction method of multipliers (PJ-ADMM) is proposed for distribution power systems with a high penetration of photovoltaic (PV) resources coordinated with battery energy storage systems (BESS). In this context, the active and reactive power outputs of the PV are locally optimized through smart inverters to improve the grid voltage with minimum power loss. Uncertainties associated with solar energy generation and load demands are considered in the defined scenarios. This study consists of two phases. In the first phase, the voltage control problem is formulated as an optimization problem to regulate the voltages within an acceptable limit with fast convergence. In the second phase, a coordinated voltage control strategy for smart PV inverters and BESS is proposed to allocate the power capacity of the battery energy storage systems and the active power loss reduction. Finally, the proposed method is tested on modified IEEE 13-bus, 33-bus and 141-bus distribution systems using MATLAB/Simulink and MATPOWER. A comparison of the results of the voltage profiles with and without the control algorithm demonstrated the efficacy, robustness, and scalability of the distributed scheme for voltage improvement and optimal utilization of PV power under different scenarios.

INDEX TERMS Distributed energy resources (DERs), solar photovoltaic (PV), voltage control, smart inverter, multi-agent system (MAS), battery energy storage systems (BESS), optimization, proximal Jacobian alternating direction method of multipliers (PJ-ADMM).

I. INTRODUCTION

The demand for distributed energy resources (DERs) has significantly increased. Solar photovoltaic (PV) power is a promising renewable energy source in the global market [1]. Over the last decade, the development of PV sector technology has rapidly increased worldwide [2]. However, the

The associate editor coordinating the review of this manuscript and approving it for publication was Ning Kang.

penetration of PV resources has caused various challenges in the performance of low-voltage distribution networks, one of which is the voltage violation issue due to the mismatch between loads and solar PV generation [3]. Moreover, uncertainties associated with the intermittent nature of PVs lead to additional challenges in balancing the power and voltage profiles of the system [4].

Various methods have been proposed to prevent and overcome voltage problems in distribution networks, such as

IEEE Access

S. R. Far et al.: ADMM-Based Multi-Objective Control Scheme for Mitigating the Impact of High Penetration DER Integration

1) upgrading the grid by installing more infrastructure, such as cables, which is usually costly [5], 2) using control devices, such as capacitor banks and on-load tap changers, which are not sufficiently fast to regulate the voltage in highly penetrated networks [6], and 3) PV power curtailment during high-power generation is an effective strategy. However, active power curtailment causes a loss of PV energy capacity, which is against the decarbonizing goals [7].

With the recent update of the IEEE 1547 standard [8], intelligent PV inverters can provide more features in grid voltage support through their active power control (Volt-Watt) and reactive power control (Volt-VAr) functions [9]. Smart inverters can regulate voltage by curtailing active power [10]. The reactive power control functions of the smart inverter can also support the voltage by supplying or absorbing reactive power [11]. These advanced features provide more flexibility in voltage support and enable smart inverters to play an active role in maintaining the stability of the distribution grid. Additionally, smart inverters can have communication lines that allow them to receive reference active and reactive power from the grid operator, which can be used to further optimize and coordinate their output to support the grid voltage.

Different techniques have been studied in the literature for controlling the voltage in the distribution network, which is categorized based on their architectures:1) centralized, 2) decentralized, and 3) distributed multi-agent systems (MAS) control [13]. A centralized control scheme with multiple DERs typically addresses challenges in terms of scalability. In the centralized control method, a central controller is required to regulate the voltage profile of the network. However, centralized control structures face communication challenges in large-scale networks. Moreover, this control architecture can result in single-point failures [14]. A centralized control method was formulated for a distribution network in [15] to control battery energy storage systems, overcome the voltage rise issue, and reduce power costs. However, owing to a lack of coordination among agents in case of failure, other agents do not support the system. Therefore, the entire system failed.

The second category is the decentralized control method. Each unit processes local data in this technique without interacting with the other units [16]. Therefore, this scheme cannot achieve optimal management. The authors in [17] developed a decentralized power control scheme for PV units that uses only their local computations to minimize the total cost of power losses and results in closed-form updates per node. Coordinated control for PV and battery energy storage based on a decentralized structure was implemented in [18] to improve overvoltage. However, this scheme does not provide optimal management. A decentralized control framework is presented in [19] for a multi-objective microgrid in a distribution system; uncertain supply and demand parameters were modelled to address the uncertainty conditions using a robust optimization method. However, the network's constraints were not considered in the proposed scheme.

Recently, distributed control structures have attracted increasing attention. Considering the complexity of distributed energy resources, traditional distribution systems are moving towards multi-agent designs [7]. In this method, each decision-maker is called an agent, and each agent is responsible for managing its local resources and participating in data sharing in parallel with other agents [20]. Moreover, this control method has a good potential for use in the high penetration of renewable systems with several agents, as they are robust and scalable. In this control method, failure in a unit will never cause a global blackout in the network. Distributed control algorithms are mainly designed based on an iterative theoretical framework, such as the alternating direction method of multipliers (ADMM) [21], which can extract a set of optimal solutions for the optimal regulation of multiple objectives. The standard ADMM is mainly applied as an efficient solver for optimization problems with several independent objective functions [22]. A robust distributed multi-objective control technique for grid support was proposed in [21], which addresses the worst-case scenarios associated with the uncertainties of each agent using the ADMM algorithm. The authors of [23] developed a fully optimization-based distributed technique for managing local resources in multiple interconnected microgrids. In this method, the uncertainty penalties in the system can be determined locally by each unit to optimize the operation of the grid.

Reference [24] implemented the ADMM algorithm to decompose a complex nonconvex problem into several subproblems to overcome the computational complications caused by the high penetration of DERs in an extensive network. Distributed voltage control based on the ADMM was introduced in [25] with reactive power management, considering the optimal global solution for a nonconvex system. Reference [26] compared the performance of the ADMM algorithm in tests related to the optimal power flow with other decomposition algorithms. In [27], a distributed voltage control based on the consensus ADMM was developed to control the voltage in wind turbines using reactive power. In [28], an ADMM-based method was proposed to solve the power flow in a distributed system. The technology behind smart inverters actively supports the grid and handles voltage violations during undervoltage and overvoltage periods by supplying or absorbing reactive power [29].

Despite the advantages of the ADMM algorithm, its implementation has some challenges owing to its complexity. Another challenge in iterative optimization algorithms is to solve the problem within a reasonable time, which can be achieved by fast convergence [30]. A Jacobian-based ADMM algorithm was developed in [31] for voltage control by optimizing the active and reactive power support through peer-to-peer communication protocols. The communication layers were distributed between the initial control parameters and Lagrangian multipliers between the control units. In this context, a MAS-based optimization scheme can be

S. R. Far et al.: ADMM-Based Multi-Objective Control Scheme for Mitigating the Impact of High Penetration DER Integration

IEEE *Access*

formulated to improve the voltage profile of the network through parallel coordination of the smart inverter. This method aims to optimize the PV inverter outputs in the fast MAS concept to maintain the voltage within an acceptable range by utilizing reactive power support and minimum active power curtailment.

The authors in [32] proposed a convex relaxation framework as a distributed solution for the power flow problem using the Jacobi-proximal alternating direction method of multipliers (JP-ADMM) algorithm [33] which is implemented to efficiently solve the problem with fast convergence using the second-order moment relaxations provides a tighter relaxation in complex computation. The scalability of the proposed algorithm is addressed through case studies with thousands of buses. The authors in [34] present the use of a distributed power optimization technique, the JP-ADMM algorithm, to optimize the allocation of charging services for Plug-in Electric Vehicles (PEVs) and capacity for large-scale PEV charging in power distribution systems with high PEV penetration. A novel optimization approach for large-scale distributed battery units is presented in [35], which utilizes a modified version of the PJ-ADMM algorithm to optimize cost and provide flexibility services. The proposed method is demonstrated to generate optimal, real-time scalable solutions through a case study, which are equivalent to centralized optimization, and computed faster.

The primary advantage of using the PJ-ADMM algorithm is its ability to solve large-scale optimization problems with the cooperation of multiple agents in a parallel and distributed manner. The PJ-ADMM algorithm can effectively handle both convex and non-convex problems with general constraints, and it has been shown to have fast convergence and good scalability. We chose to use PJ-ADMM in this study because it can address the multi-objective and multi-agent nature of the proposed optimization problem in a distributed manner and reduce the communication burden among agents. The use of smart inverters allows for a distributed and parallelized approach to voltage control, as each inverter can work on its own subproblem independently and in parallel with the other inverters.

In this work, we focused on multi-agent distributed voltage control systems. The main motivation for conducting this study is to address the challenges posed by the high penetration of PV resources in distribution networks, specifically the voltage violation issue due to the mismatch between loads and solar PV generation, and uncertainties associated with the intermittent nature of PV generation. The study aims to provide a robust and scalable control technique that can handle the high penetration of DERs in an extensive network using the JP- ADMM algorithm for voltage control by optimizing the active and reactive power support in a large-scale network.

This study ensured the optimal utilization of PV power by controlling smart PV inverters locally using utilizing reactive power support and minimum active power curtailment

through the PJ-ADMM algorithm to distribute a centralized voltage control problem as it features a parallel updating process, rapid convergence, the capability to impose constraints, and superior global convergence performance. The application of additional penalty factors resulted in faster voltage convergence. However, curtailing the active power affects PV owner revenue by limiting the solar PV power capacity. Hence, there is still a need of designing an optimization-based distributed voltage control based on the PJ-ADMM algorithm that enjoys a fast convergence rate without power loss. This is made possible by utilizing energy storage systems to store excess energy generated by PVs during periods of low demand, which can then be released during peak demand hours.

One way to control BESS is by integrating them with smart PV inverters, allowing for adjustments to energy output in response to voltage violations on the grid. The power loss in the PJ-ADMM algorithm motivates studying the implementation of virtual storage in the PJ-ADMM algorithm and how to charge/discharge to minimum BESS sizing can be allocated. Thus, the idea of storage sizing comes from a virtual curtailment strategy through the PJ-ADMM algorithm cycle by modifying the storage participation in voltage regulation, which gives rise to the efficient utilization of the BESS capability during power imbalance periods and the reduction of power losses. The distributed control policies assign storage capacity and estimate the minimum amount of power absorbed by storage, while taking into account technical limitations such as capacity and determining the charge/discharge power to be exchanged by buses.

To the best of our knowledge, this study is the first to investigate the use of the PJ-ADMM algorithm for voltage control in high-penetration PV systems with BESS in a fully distributed structure and with power loss reduction as the main objective. The proposed method operates in two phases under different scenarios. In the first phase, the voltage control problem is formulated as a multi-objective optimization method. In the second phase, the BESSs are integrated with smart PV inverters to store excess solar power and control voltage. The control policies considered determine the active and reactive powers of the PV inverters and the charge/discharge power of the batteries. The key contributions of the study are:

- Optimal PJ-ADMM-based modulation strategy for active and reactive powers to improve voltage and meet load demand using smart inverters during day and night.
- Minimization of active power curtailment through the use of smart inverters, which provide voltage support during overvoltage conditions with reactive power contributions in a distributed manner.
- Analytical approach for coordinating PJ-ADMM with BESS for smart PV inverters to maximize PV power participation in multi-agent systems, considering network uncertainty.

- Method for optimal BESS sizing to maximize PV power utilization with PJ-ADMM for power loss reduction.
- Framework for demonstrating the scalability of the proposed algorithm in large-scale, complex distribution power systems.

The remainder of this paper is organized as follows. Section II presents a formulation of the voltage problem. Section III provides an overview of the ADMM control scheme. Section IV, the proposed control scheme includes the PJ-ADMM algorithm, and BESS sizing is considered. Section V describes the case studies. Furthermore, simulation results are presented and discussed in Section V to verify the effectiveness of the proposed algorithm in different scenarios. Finally, Section VI concludes the paper.
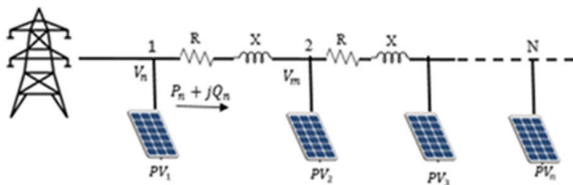

FIGURE 1. The basic structure of a distribution system with multiple PV agents.

II. PROBLEM FORMULATION

Fig. 1 shows the basic structure of a distribution system with several agents. The objective function of the voltage control problem based on a centralized system is represented in (1a), which aims to minimize the costs of changes in the active power (P) and reactive power (Q) of PV inverters at time step t.

$$\text{Minimize}_{\Delta P, \Delta Q} \sum_{n \in N} F_n^P (\Delta P_n^{(t)})^2 + F_n^Q (\Delta Q_n^{(t)})^2 \quad (1a)$$

$$\text{Subject to} : V^{min} \leq V_n^t \leq V^{max} \quad \forall n \in N \quad (1b)$$

where N is the set of PV inverters installed in the system, and n is the number of contributed inverters. The variables $\Delta P_n^{(t)}$ and $\Delta Q_n^{(t)}$ refer to the changes in the active and reactive powers of the nth inverter, respectively. $F_n^P (\Delta P_n^{(t)})^2$ and $F_n^Q (\Delta Q_n^{(t)})^2$ are the cost functions associated with changes in the active and reactive powers of the inverters, respectively. F_n^P and F_n^Q are constant penalty factors that denote the control of participation, P and Q, respectively. In this regard, each inverter must locally satisfy the voltage constraint (1b). V^{min} and V^{max} denote the lower and upper voltage bounds of the nth PV inverter, respectively. Constraints (1c) and (1d) on variables $\Delta P_n^{(t)}$ and $\Delta Q_n^{(t)}$ are considered for model (1a) to maintain the lower and upper limits on the voltage magnitude of the units and to constrain the amount of exchanged power between the nodes. V_n^t represents the nth inverter voltage magnitude at the point of common coupling (PCC) after applying $\Delta P_n^{(t)}$ and $\Delta Q_n^{(t)}$.

$$(-C_u)(P_i^{PV})^{(t)} \leq \Delta P_n^{(t)} \leq 0 \quad (1c)$$

$$-(\Delta Q_n^{(max)})^{(t)} \leq \Delta Q_n^{(t)} \leq (\Delta Q_n^{(max)})^{(t)} \quad (1d)$$

The active power curtailment factor is denoted as $C_u.(P_n^{PV})^t$ is the power generated by the nth inverter. The apparent power is denoted as S_n. The maximum reactive power curtailment can be calculated through (1e):

$$(\Delta Q_n^{(max)})^{(t)} = \sqrt{S_n^2 - ((P_n^{PV})^t + \Delta P_n^{(t)})^2} \quad (1e)$$

$$f(V_n^t, \Delta P_n^{(t)}, \Delta Q_n^{(t)}) = 0 \quad (1f)$$

where constraint (1f) denotes the nonlinear relation between the voltage magnitude and the active and reactive powers as input variables in each inverter, which causes nonconvex power flow problems [33]. The linearization of all voltage magnitudes using voltage sensitivities can help formulate a linear relationship between the input parameters to solve the power flow problem in the convex relaxed form in the distributed scheme [27]. The relation between the bus voltage magnitude and small variations in the active and reactive powers for a set of inverters can be calculated using voltage sensitivities. A first-order approximation can be used, as shown in equation (2):

$$V_m^{(k)} \approx \left(V_m^{(M)}\right)^{K-1} + \sum_{n \in N} \frac{\partial V_m}{\partial P_n} \Delta P_n^{(k)} + \frac{\partial V_m}{\partial Q_n} \Delta Q_n^{(k)} \quad (2)$$

where $\Delta P_n^{(k)}$ and $\Delta Q_n^{(k)}$ denote the deviations in the active and reactive powers in each iteration k. $\left(V_m^{(M)}\right)^{K-1}$ denotes the measured voltage of bus m at the previous iteration (k-1). $\frac{\partial V_m}{\partial P_n}$ and $\frac{\partial V_m}{\partial Q_n}$ are the voltage sensitivity coefficient matrices updated at each node in each iteration [36]. These parameters express the influence of changes in variables P and Q on the voltage control of the inverters and can be written in simplified forms $\frac{\partial V_m}{\partial P_n} \approx V_{nm}^{(P)}$ and $\frac{\partial V_m}{\partial Q_n} \approx V_{nm}^{(Q)}$. It is possible to express equation (2) as follows:

$$V_m^{(k)} \approx \left(V_m^{(M)}\right)^{K-1} + \sum_{n \in N} V_{nm}^{(P)} \Delta P_n^{(k)} + V_{nm}^{(Q)} \Delta Q_n^{(k)} \quad (3)$$

The topology of the grid and the information about the line impedances can be used to compute the voltage sensitivity coefficients. For a set of inverters, a linear voltage model can be expressed using the voltage sensitivity coefficients ($V_{nm}^{(P)}$ and $V_{nm}^{(Q)}$), which represent the effect of active and reactive power, respectively, on the controlled voltage.

In this regard, the optimization problem is solved by a centralized design by gathering variables as inputs, such as solar power generation and bus voltage, to solve the problem, and a central optimizer minimizes the total change in active/reactive power in each inverter to achieve the optimal control in the system. The central controller then shares the new set of points with all agents to support the grid. However, the major challenge of this method is that the system is always at risk of a single point of failure. A central coordinator is required to collect variables from each unit to regulate an optimal set point for supporting the grid. In this scheme, a robust communication system is also required to exchange information between the agents participating in the system. Therefore, a solution to the challenges above is to

S. R. Far et al.: ADMM-Based Multi-Objective Control Scheme for Mitigating the Impact of High Penetration DER Integration

IEEE *Access*

use a method to split the centralized control system into a multi-block control system that can improve the voltage profiles in parallel using MAS-based algorithms.

III. ADMM APPROACH

The ADMM algorithm was originally a system with two blocks, which has been widely applied to solve distributed optimization problems in different applications. However, it is desirable to partition the centralized optimization problem into multiple agents that allow parallel computing to solve problems in large-scale distribution systems [37]. In general, a convex optimization problem is expressed as follows [21]:

$$\text{Min } A(x) + B(z) \tag{4a}$$
$$\text{Subject to : } ax + bz = c \tag{4b}$$

where $A(x)$ and $B(z)$ are independent objectives and separable considering variables x and z, equation (4c) can be formulated to solve the optimization problem using the augmented Lagrangian function with penalty terms [38], where ρ the augmented penalty factor on the constraints is a constant positive factor.

$$L_\rho^{(x,z,\lambda)} = A(x) + B(z) + \lambda^T(ax + bz - c)$$
$$+ \frac{\rho}{2}||ax + bz - c||_2^2 \tag{4c}$$

Finally, the ADMM model of (4a) is derived in (4d)-(4f) when the variables are updated in each iteration k, as follows [21]:

$$x^{k+1} = \arg\min L_\rho(x, z^k, \lambda^k) \tag{4d}$$
$$z^{k+1} = \arg\min L_\rho(x^k, z, \lambda^k) \tag{4e}$$
$$\lambda^{k+1} = \lambda^k + \rho\left(ax^{k+1}, bz^{k+1} - c\right) \tag{4f}$$

Although the standard ADMM performs well in solving convex models, its performance in terms of convergence is insufficient for non-convex problems. In this regard, the multi-block ADMM can be advanced to the proximal Jacobian ADMM to relax the coupling between the functions and help decompose the centralized problem into several minor problems [30], [39]. This study proposes a MAS-based distributed control system for voltage regulation using a distributed optimization algorithm. Applying the PJ-ADMM approach, the centralized problem can be decomposed into subproblems that can be updated in parallel to be solved by each agent with fast convergence iteratively [40].

IV. CONTROL SCHEME

A. PJ-ADMM ALGORITHM

The PJ-ADMM is selected to solve the proposed optimization problem because of its robustness and high performance in determining optimal values compared to other ADMM-based algorithms. The original proximal Jacobian ADMM methodology was adapted from [33]. The centralized objective function in (1a) can be decomposed into the sum of

several convex functions related to each PV unit considering the local constraints. In each iteration, the variables ΔP and ΔQ are updated in parallel. Adding proximal terms such as penalty factors helps speed up the convergence rate. Equation (6) is a derivation of the proximal augmented Lagrangian of the (1a) after adding proximal terms on each sub-problem and considering the initial limits on variables $V_n^k, \Delta P_n^{(k)}$ and $\Delta Q_n^{(k)}$ in (1b)- (1f) is given formulated in (6):

$$f_n^k = F_n^P(\Delta P_n^{(k)})^2 + F_n^Q(\Delta Q_n^{(k)})^2 \tag{5}$$

$$\mathcal{L}_\rho(\Delta P_n^{(k)}, \Delta Q_n^{(k)}, (\lambda_n^{max})^{(k-1)}, (\lambda_n^{min})^{(k-1)})$$
$$= \Sigma(f_n^k + (\lambda_n^{max})^{(k-1)}\left(V_n^k - V^{max}\right)$$
$$+ (\lambda_n^{min})^{(k-1)}\left(-V_n^k + V^{min}\right)$$
$$+ \frac{\rho_n}{2}\max(0, \left(V_n^k - V^{max}\right))^2$$
$$+ \frac{\rho_n}{2}\max(0, \left(-V_n^k + V^{min}\right))^2$$
$$+ \frac{\tau_n}{2}(\Delta P_n^{(k)} - (\Delta P_n^c)^{(k-1)})^2$$
$$+ \frac{\tau_n}{2}(\Delta Q_n^{(k)} - (\Delta Q_n^c)^{(k-1)})^2) \tag{6}$$

where λ_n^{min} and λ_n^{max} denote the Lagrangian multipliers corresponding to the constraints on the nth inverter control variable. τ_n is the proximal penalization factor associated with the proximal terms $(\Delta P_n^{(k)} - (\Delta P_n^c)^{(k-1)})^2$ and $(\Delta Q_n^{(k)} - (\Delta Q_n^c)^{(k-1)})^2$ on each subproblem. The subscript c refers to constant values. This parameter is used to ensure the convergence of the controlled voltage. The proposed approach enjoys fast convergence by adding proximal terms to the control variables P and Q deviation. The objective functions can be distributed to each PV inverter and coordinated locally and in parallel with other controllers. The equation of the proximal Jacobian version of the ADMM for local controllers in a multi-agent network can be derived in (8).

$$H_{nm}^{(k)} = \Delta P_n^{(k)}V_{nm}^{(P)} + \Delta Q_n^{(k)}V_{nm}^{(Q)} \tag{7}$$

$$\mathcal{L}_n^{PJ-ADMM} = f_n^k + \Sigma(((\lambda_n^{max})^{(k-1)} - \left(\lambda_n^{min}\right)^{(k-1)})H_{nm}^{(k)}$$
$$+ \frac{\rho_n}{2}\max(0, \left((V_n^M)^{(k-1)}\right) - V^{max} + H_{nm}^{(k)})^2$$
$$+ \frac{\rho_n}{2}\max\left(0, \left(-(V_n^M)^{(k-l)}\right) + V^{min} - H_{nm}^{(k)}\right)^2)$$
$$+ \frac{\tau_n}{2}(\Delta P_n^{(k)} - (\Delta P_n^c)^{(k-1)})^2$$
$$+ \frac{\tau_n}{2}(\Delta Q_n^{(k)} - (\Delta Q_n^c)^{(k-1)})^2)) \tag{8}$$

$$\tau_n > \rho_n\left(\frac{|D|}{2 - U_n} - 1\right) \tag{9}$$

By applying the PJ-ADMM algorithm, the original optimization problem of the system can be partitioned into several subproblems. These subproblems are formed based on the constraints of the problem, and they are distributed among different agents. In a multi-agent control system, each agent

is responsible for solving a specific subproblem that is part of the overall optimization problem. The subproblems are typically related to the control of a specific aspect of the system, such as voltage regulation in the case of the inverters mentioned in this paper. The agents optimize their local subproblems while sharing information with other agents to ensure the global solution is obtained. The subproblems are typically designed to be solved independently, with each agent having its own set of decision variables and local constraints. The solutions from each agent are then combined to form a solution for the overall optimization problem. This approach allows for a distributed and parallelized solution to the optimization problem, as each agent can work on its own subproblem without needing to communicate with every other agent.

In the context of this paper, each agent in the multi-agent control system is a smart inverter. The inverters are equipped with voltage-support functions and are responsible for solving a specific subproblem related to the control of voltage within the system. The inverters work together to maintain the overall voltage within limits, and the solutions from each inverter are combined to form a solution for the overall optimization problem.

Once the voltage of any agent is outside the constraints, the model operator can return the values to the required range and minimize active power loss by optimizing the control variables. Furthermore, to improve the convergence speed of the voltage, proximal penalty factors and additional acceleration terms are used in the PJ-ADMM algorithm. This study used the acceleration factor U_n for fast updating in Lagrangian multipliers, which led to fast convergence. The condition for the parameter τ is given by (9), where τ depends on the number of inverters in the system, the acceleration factor, and the proximal penalization factor. For a set of inverters, a smaller τ provides faster convergence in the voltage control.

The details of the multi-block PJ-ADMM scheme are summarized in Algorithm 1. Here, V^M corresponds to the voltage measured at the PCC for a set of inverters after applying small changes in P and Q at each iteration. It should be noted that the voltage control scheme has an iterative manner. In each round k, the control system regulates the inverter's active and reactive powers and PCC voltage, followed by updating the Lagrangian multipliers.

B. BESS OPTIMAL SIZING FOR POWER LOSS REDUCTION
Energy storage has been identified as a valuable approach for addressing the issue of load mismatch and incorporating renewable energy. In recent years, battery energy storage systems have become a significant choice among energy storage technologies due to their notable improvements in terms of both performance and cost-effectiveness. During the charging mode, BES systems can act as a load by receiving energy from the grid to charge its batteries. However, in the discharging mode, BES systems can act as a generator by releasing stored energy to the grid, thus providing a source of energy.

Algorithm 1 PJ-ADMM Coordinated With BESS

Phase I:

Initialize the variables ΔP, ΔQ, λmax, and λmin. Set the voltage V at each node to 0.

Measure the voltage at the Point of Common Coupling (PCC).

If the voltage is within the specified constraints:

$V^{min} \leq V^M \leq V^{max}$, then begin the local control iterations.

For k = 0, 1, …, d, update the active power deviation ΔP and the reactive power deviation ΔQ in each subsystem by solving the optimization problem given by:

$$\text{argmin}_{\Delta p, \Delta q} \mathcal{L}_n^{PJ-ADMM}$$

Send the calculated values of ΔP and ΔQ to the control cycle of each inverter.

Constrain the values of ΔP and ΔQ by the following conditions:

$$(-C_u)(P_n^{PV})^{(k-1)} \leq \Delta P_n^{(t)} \leq 0$$
$$-(\Delta Q_n^{(max)})^{(k)} \leq \Delta Q_n^{(k)} \leq (\Delta Q_n^{(max)})^{(k)}$$

Update the variables λmax and λmin for each agent in parallel as follows:

$$(\lambda_n^{max})^{(k)} = \max(0, (\lambda_n^{max})^{(k-1)} + \rho_n U_n((V_n^M)^{(k)} - (V)^{(max)})$$
$$(\lambda_n^{min})^{(k)} = \max(0, (\lambda_n^{min})^{(k-1)} - \rho_n U_n((V_n^M)^{(k)} - (V)^{(min)})$$

End

Phase II:

For each hour h = 0, 1, …, 24, repeat the following steps:

For each BESS, Bn = 0, 1, …, 4, absorb or inject ΔP to/from the BESS.

For all BESS, update equations (16) and (17) to determine the charging/discharging active power.

Update the charging power $P_{B_d,h}^{charge}$ and discharging power $P_{B_d,h}^{Discharge}$ in the optimization cycle.

Measure the voltage at the PCC.

If the voltage is within the specified constraint:

$V^{min} \leq V^M \leq V^{max}$, then end the iteration.

Determine the required BESS capacity and charging/discharging rates.

In this study, by the end of Phase I, the minimum required active power curtailment, denoted by ΔP, for voltage-rise mitigation is computed using the PJ-ADMM algorithm. This section focuses on a robust optimization-based voltage control technique through the PV-battery coordination model of a distribution system dominated by PV systems, where the curtailed powers are specified for the charging or discharging operations of the BESS to regulate the voltage profiles. The model is developed aims to overcome the overvoltage and power loss challenges that arise with the high integration of PVs. The control scheme consists of a multi-agent control algorithm and the voltage control problem is defined as an optimization problem. In this technique, the agents

S. R. Far et al.: ADMM-Based Multi-Objective Control Scheme for Mitigating the Impact of High Penetration DER Integration

IEEE *Access*

coordinate with each other to estimate the required amount of curtailing active power and storage sizing needed to modulate the voltages rise.

In the presence of uncertainties, once a voltage violation is detected in any node, the optimization control algorithm will be active in computing the minimum amount of active power curtailment required to mitigate the voltage violation. Therefore, the charging power of the BESS at each hour of running the optimization algorithm is the same as the curtailed active power of the PVs. To comply with network constraints, providing energy at an optimal rate is of great significance. The aim is to allocate BES for maximum benefits from discharge mode. The control cycle considered in this methodology is included active power curtailment from PV inverters and charge/discharge power from virtual storages in the control cycle of the algorithm. This method will contribute to keeping the power grid balanced by smoothing out the demand peaks through the algorithm coupling the BESS with PV inverters and improving the local consumption during the low-demand periods in the distribution system. When the load demand exceeds the generated PV power, the BESS starts to discharge.

In this way, the active power of PV inverters will be cut by saving the excess active power in the storage which helps alleviate the voltage rise issue in high PV generation periods. In peak load periods, the stored energy in BESS will be used for improving the voltage profile of the grid during voltage drop periods. The general structure of the proposed optimization method is shown in Fig 2. The coordinated voltage control policy determines storage integration into the voltage profile. In this case, the reactive power of the BESS is not considered in the optimization cycle. The participation of storage systems is proportional to their capacity, based on the load demand at that hour of the day. The results show how the developed mathematical optimization algorithm allocates BESS capacity to voltage control.
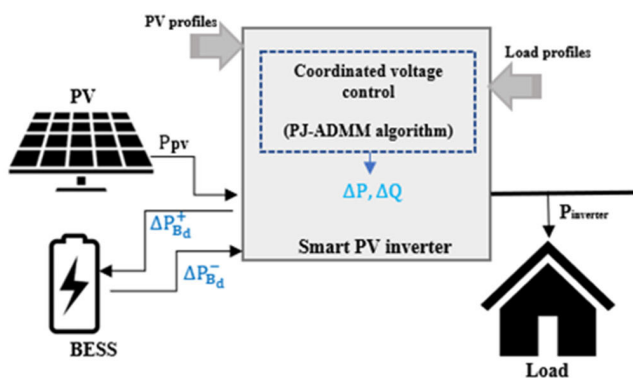

FIGURE 2. General overview of the coordinated voltage control system.

The BESS is subject to charging power P_{charge}^t and discharging power $P_{discharge}^t$ constraints. The stored power of the battery system at any time step t should not surpass the considered limits. The boundary on the power charging and discharging can be represented as equations (10) -(12) where P_{max} is the maximum charge/discharge power.

$$0 \leq P_{charge}^t \leq P_{max} \tag{10}$$

$$0 \leq P_{discharge}^t \leq P_{max} \tag{11}$$

$$P_{charge}^t \cdot P_{discharge}^t = 0 \tag{12}$$

These constraints enforce that the power output of the BESS cannot surpass its power capacity. Constraint (13) enforce that the energy stored in the batteries should be maintained within an acceptable range to avoid excessive charging/discharging and increase the battery's longevity.

$$E_{min,Battery} \leq E_{Battery}(t) \leq E_{max,Battery} \tag{13}$$

In the given context, t represents the overall number of time intervals over the control horizon. $E_{Battery}(t)$ signifies the energy level of at time t. $E_{max,Battery}$ and $E_{min,Battery}$ denote the upper and lower bounds of its energy capacity, respectively. The amount of energy stored in each battery can be calculated by using the following equation (14):

$$E_{Bat}(t+1) = E_{Bat}(t) + (P_{charge}(t)\eta_{ch} - P_{discharge}(t)/\eta_{dch})\Delta t \tag{14}$$

Note that there are some charging/discharging losses in the batteries owing to the internal resistance, which is modelled by introducing the charging/discharging efficiency of the batteries with η_{ch} and η_{dch}. These values can vary depending on the case study and have been approximated in different ways. They can be a single constant value, or as functions of the charging/discharging rate of BESSs. However, a linear relationship exists between the charging efficiency and the charging rate as given in (15). The BES can be described using constant coefficients α and β. The same approach can be applied to the discharging mode.

$$\eta_{ch} = \alpha_n - \beta_n P_{charge} \tag{15}$$

In the case, if this study, the equations (16) and (17) are shown the active power charging and discharging of the nth battery at bus d, where $B_{n,d,h}$ is the set of BESS installed in the system for 24 hours each time step h.

$$P_{B_{n,d,h}}^{charge} = \eta_{ch} \times \Delta P_{B_{n,d}}^+ \tag{16}$$

$$P_{B_{n,d,h}}^{Discharge} = \Delta P_{B_{n,d}}^- / \eta_{dch} \tag{17}$$

Here, $P_{B_{d,h}}^{charge}$ and $P_{B_{d,h}}^{Discharge}$ are the actual power absorbed and injected by the nth BESS, respectively, and the charging/discharging active power of the nth BESS at bus d is equal to $\Delta P_{B_{n,d}}^+$ and $\Delta P_{B_{n,d}}^-$ respectively. The energy stored in each BESS is selected to equal its capacity, considering the efficiency of 95%. $\Delta P_{B_{n,d}}^+$ and $\Delta P_{B_{n,d}}^-$ are assumed to be the active power deviations (pu). Their sign is considered to be either positive or negative, depending on the BESS operating mode. When the battery operates in the charging mode, ΔP is positive. When the battery works in the discharging mode,

IEEEAccess

S. R. Far et al.: ADMM-Based Multi-Objective Control Scheme for Mitigating the Impact of High Penetration DER Integration

ΔP is negative. The algorithm determines which BESs from the network are chosen to participate in the control cycle and how much power is charged or discharged to satisfy the voltage control constraints over the whole network.

V. CASE STUDY

In this section, the performance of the proposed algorithm is validated using small systems such as modified IEEE 13-bus and 33-bus distribution feeders. The scalability of the proposed method is demonstrated with the IEEE 141-bus distribution feeder. The optimization problem is solved using YALMIP [41]. Simulations of the 13-bus system are performed using MATLAB/Simulink 2021b and executed on a PC with an Intel i7-4790 3.60 GHz CPU and 16 GB RAM. The MATPOWER package 7.0 [42] is used for the method's power flow and voltage analyses on the 33-bus and 141-bus systems. The proposed method combines locally distributed voltage control based on the PJ-ADMM and the charge/discharge of batteries. The validation then focuses on the effect of the implemented method in satisfying decarbonization goals, such as minimum power loss, maximizing the participation of PVs capacity, and satisfying load demands under different conditions to maintain the voltages of all buses and PV/battery inverter constraints within an acceptable rage.

A. 13-BUS SYSTEM

The modified configuration of the IEEE 13-bus test feeder with the PV locations is illustrated in Fig. 3. Four PV panels with similar solar irradiance profiles and commercial load profiles with a capacity of 200 kW were installed on buses 634,675,692 and 684. The ratios of PV generation to load during peak hours are listed in Table 1. The detailed data of the loads and solar power profiles were adapted from [43] and modified based on the capability of the system used in this case study. Using the MAS-based topology, each inverter is an independent agent. All participating inverters are smart and operate with voltage-support functions. Each PV unit's active and reactive powers are regulated in each round of the optimization calculation cycle. In addition, uncertainties

FIGURE 3. The 13-bus distribution network.

TABLE 1. The ratio of PV generation compares to the load during peak hours.

Time(h)	PV/Load %
11:00	28%
12:00	31%
13:00	25%

regarding the PV power and load disturbances are considered in the case studies. The system parameters are shown in p.u. The voltage constraint in each bus is set to [0.95, 1.05] p.u. Finally, the iteration number is considered to investigate the influence of related parameters on the convergence rate.

In this study, four possible scenarios are considered to indicate the effectiveness of the proposed control strategy. The performance of the implemented method at all smart inverters is analyzed when the system is experiencing under or upper voltage conditions, specifically at midday and early at night. An advantage of the proposed algorithm is that it improves the voltage profiles with a minimum amount of reactive power compensation and active power curtailment at each iteration. The performance of the proposed optimization method is compared with that of the base case without distributed control. The grid voltage support function does not need to be activated when the voltage falls below the limits.

Several parameters of the algorithm influenced the results. The term C_u is used to penalize active power curtailment. In this study, C_u is set to 1, which means that the inverters can curtail the maximum capacity of their active power when necessary. The active and reactive power penalization factors are $F_P = 1000$ and $F_Q = 500$ (based on trial and error). Here, $F_P > F_Q$ for minimizing active power curtailment. The number of iterations is related to the penalty factor F_P. Generally, small F_P yields a faster convergence. We also examined the effects of τ on the convergence speed.

B. SCENARIO I

Scenario I involve only active power control by curtailing the active power to reduce overvoltage when the PV output reaches its maximum value. Fig. 4(a)-4(c) presents the 24-hour voltage profile of the network with the proposed controller under scenarios I and II compared with the profile without control. Fig. 4 (a) shows the voltage profiles of the buses without control. The yellow line indicates the maximum boundary at Vmax = 1.05 p.u. It can be observed that the voltage rise problem occurs when there is low load demand and high PV generation. It can be observed that the voltage violates the upper limit on some buses in the time slots of 11:00-13:00. As shown in Fig. 4 (a), the voltages on bus 634 exceeded the constraints, with a voltage of 1.053 at midday. The inverter at the end of the line at bud no 634 is selected to monitor the method's performance because it
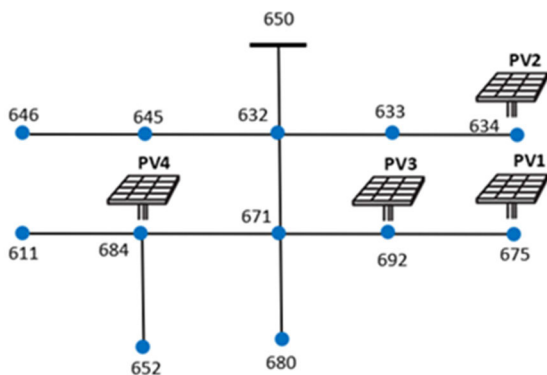
S. R. Far et al.: ADMM-Based Multi-Objective Control Scheme for Mitigating the Impact of High Penetration DER Integration

IEEE Access

TABLE 2. Results under scenario II.

Time(h)	Voltage without control (p.u.)	Voltage under scenario II (p.u.)[a]	ΔQ(kVAr)
20:00	0.983	1.013	20.208
21:00	0.985	1.012	20.215
22:00	0.986	1.012	20.226

is more sensitive. In Fig. 4 (b), we can see that using the PJ-ADMM algorithm, the voltage rise problem at noon is mitigated to 1.043 through an iterative voltage regulation method.

C. SCENARIO II

The second scenario is the method of supporting voltage by reactive power in the under-voltage condition when the voltage of some nodes is lower than 1 p.u. during 1:00-16:00 and 18:00–24:00. In this scenario, there is no need to afford active power control. As shown in Fig. 4 (c), when there is no PV generation and high load demand in the early evening, all buses experience low voltages. In this case, injecting reactive power can improve the voltage profile.

In this scenario, we set the constraint for reactive power as the maximum capacity of the inverters. The results indicate that intelligent inverters can support the grid at night by injecting reactive power. It can be seen that the voltage drop occurs at 20:00, approximately 0.98 p.u., which is improved to 1.02 pm. Table 2 lists the total amount of reactive power

FIGURE 4. (a) 24h voltage profile of the system without control, (b) voltage profile with control under the scenario I, and (c) voltage profile with control under scenarios I and II.

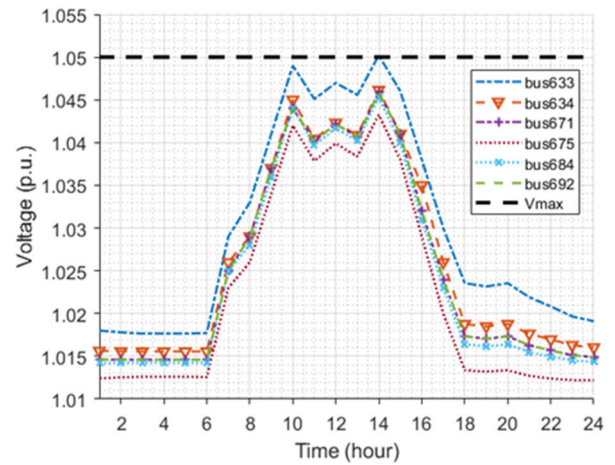provided to the inverters at bus 675 during 20:00–22:00 under scenario II.

FIGURE 5. Voltage regulation under scenario III.

D. SCENARIO III

In this scenario, active power curtailment is disabled. Therefore, the PCC voltage is regulated using only reactive power when an overvoltage problem occurs. Fig. 5 shows the optimized voltage profile under scenario III. It can be observed that the voltage rise during peak hours is controlled for all participating buses. Smart inverters start decreasing the overvoltage by absorbing a minimum amount of reactive power with no active power loss. In this case, smart inverters contribute to voltage control through a voltage support function by supplying or absorbing reactive power during voltage-rise conditions.
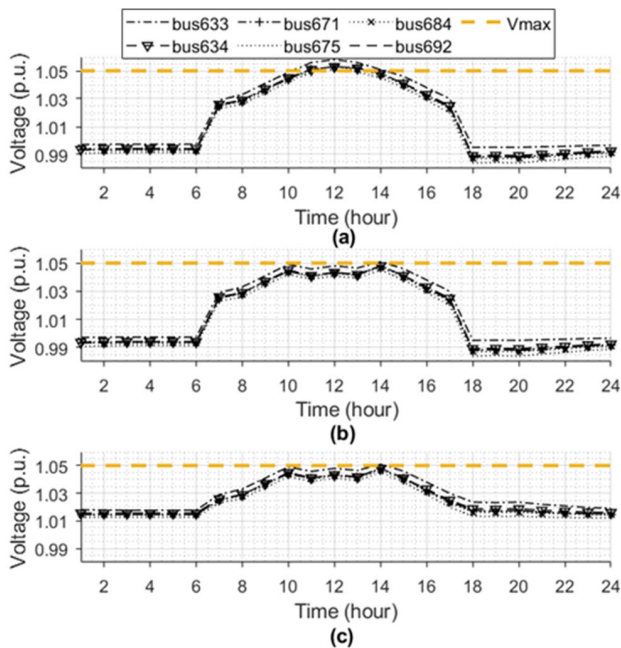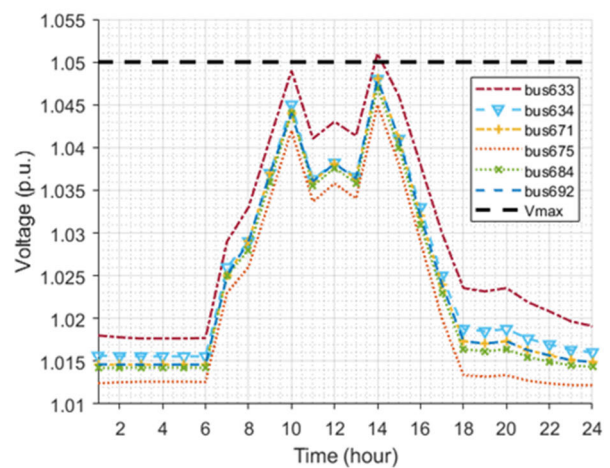

FIGURE 6. Voltage regulation under scenario IV.

E. SCENARIO IV

The last scenario is designed to verify the effectiveness of intelligent inverters in voltage profile regulation with both active and reactive powers during periods of high solar power

IEEE *Access*

S. R. Far et al.: ADMM-Based Multi-Objective Control Scheme for Mitigating the Impact of High Penetration DER Integration

generation. In this case, smart inverters provide reactive power to the grid, along with the minimum curtailment of active power at each iteration, until the desired voltage limits are reached for all buses. Fig. 6 shows the controlled voltage profiles under scenario IV.

TABLE 3. The total amount of curtailment in the system.

Time (h)	Scenario I		Scenario III		Scenario IV	
	ΔP (kW)		ΔQ (kVAr)	ΔP (kW)		ΔQ (kVAr)
11:00	27		52	23		31
12:00	32		48	24		33
13:00	24		51	26		32

TABLE 4. Active and reactive power in the swing bus at midday.

Strategy	P(kW)	Q(kVAr)
Without control	1724	1060
Scenario I	1756	1060
Scenario III	1724	1109
Scenario IV	1749	1094

Table 3 illustrates the total active and reactive power curtailment under each scenario in the entire system during 11:00 -13:00 when PVs are at maximum output. In the last scenario, the total reactive power support at noon is approximately 33 kVAR. In contrast, the entire curtailed active power when the system experiences the maximum overvoltage is about 24 kW, which shows the impact of reactive power curtailment on the voltage profile of the system. Note that there was no voltage violation for the rest of the day; therefore, the voltage support functions were inactive during these hours. Table 4 presents the active and reactive powers received from the main network under the different scenarios at 12:00. These values reflect the amount of curtailed active and reactive powers, as shown in Table 3. Note that the PVs were at their maximum generation levels at midday.

Fig. 7 shows the active and reactive power curtailment at bus-634. In this result, the performances of scenario III with only reactive power control and scenario IV with both active and reactive power curtailment are compared. Fig. 8 shows the high-speed convergence of the voltage in bus-634 at midday under the different scenarios. Notably, the voltages are returned to the range of constraints by selecting the optimal value for the acceleration factor through the proposed algorithm for each agent independently in less than ten iterations. In this case, better results were achieved when the curtailment acceleration factor was set to $Y_P = 10000$, the reactive acceleration factor was $Y_q = 100$, and the proximal penalization factor was set to $\tau = 0.0001$.

Finally, a comparison of the results shows that applying the PJ-ADMM algorithm can improve the voltage profile of the multiagent system. It can be observed that the smart inverters
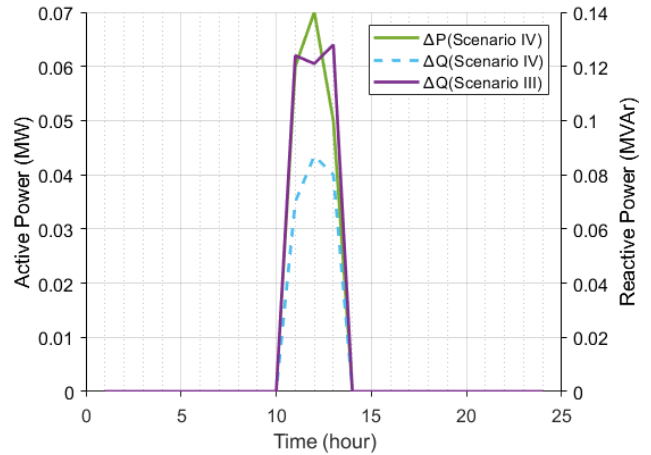

FIGURE 7. Active and reactive power curtailment at bus-634 under scenarios III and IV.

at all buses start supporting the grid voltage locally and in parallel by injection/absorbing reactive power. Moreover, both control variables P and Q are updated with minimum curtailment at each iteration in parallel for all agents. Table 5 lists the voltages in bus 634 (with PV) and bus 633 (without PV) during peak hours. As can be seen, this method can maintain the voltage of all nodes in the allowed range, considering the uncertainties in the high penetration of solar PV networks. Smart inverters can also contribute to voltage control in buses without PV with reactive power control, which shows the ability of smart inverters in voltage regulation. The results demonstrated the flexibility and capability of the algorithm in smart inverters using reactive power, which considerably impacts voltage control. Scenario IV provides optimal regulation of the voltage profile with minimum curtailment compared with the other cases.
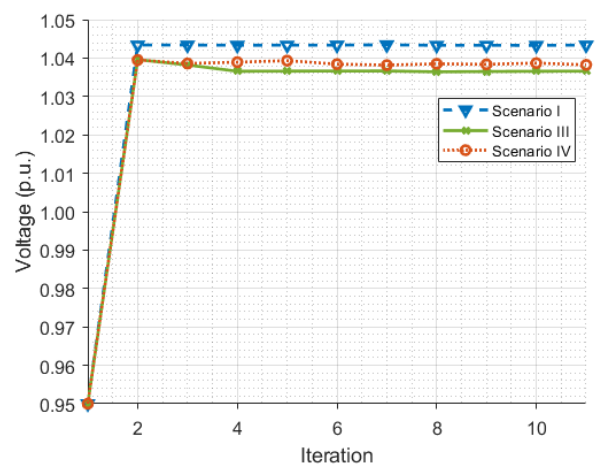

FIGURE 8. Voltage convergence at bus 634 at 12:00.

F. 33-BUS SYSTEM

The performance of the proposed scheme is tested using a 33-bus system. The MATPOWER package 7.0 was used for

S. R. Far et al.: ADMM-Based Multi-Objective Control Scheme for Mitigating the Impact of High Penetration DER Integration

IEEE Access

TABLE 5. Maximum voltage (p.u.) in buses 634 and 633 at midday.

Bus	Without control	Scenario I	Scenario III	Scenario IV
634	1.053	1.043	1.036	1.038
633	1.058	1.047	1.041	1.043

the power flow analysis and computing voltage profiles. The robust optimization problem was solved using the YALMIP toolbox. In this case, 20 PVs with an equivalent capacity of 0.2 MW were installed. Four distributed BESSs were considered in this system. Each BESS has a capacity of 2.5 MWh. A block diagram of the proposed control strategy is shown in Fig. 9, where it should be noted that all loads of the IEEE 33-node test system were increased by 10% to stress the network. The voltage constraints for each bus were set to [0.98 1.05] p.u.

Fig. 10 shows the voltage profiles of the 33-bus system without voltage control. It can be observed that the voltages violate the voltage constraints at midday and noon. This section presents the results for the optimal sizing of the BESS. In this method, voltage rise/drop problems are addressed using virtual BESSs to optimally utilize the active power of an intelligent PV inverter. Power generation from PV inverters can be limited by absorbing excess active power using batteries, which helps to reduce solar energy curtailment. The charging mode can be considered a network load, and the energy stored in the storage systems can be used as backup power during the discharging mode when the BESS provides energy to the network.
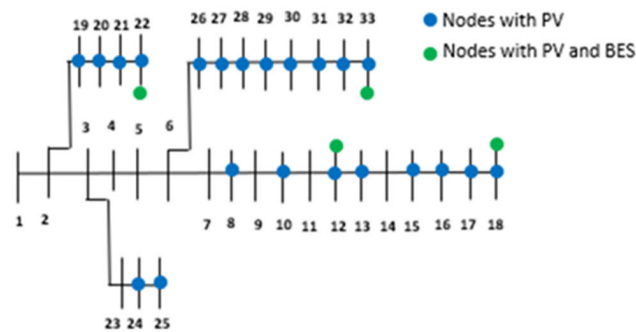

FIGURE 10. Voltage profiles of 33-bus system with no voltage control.
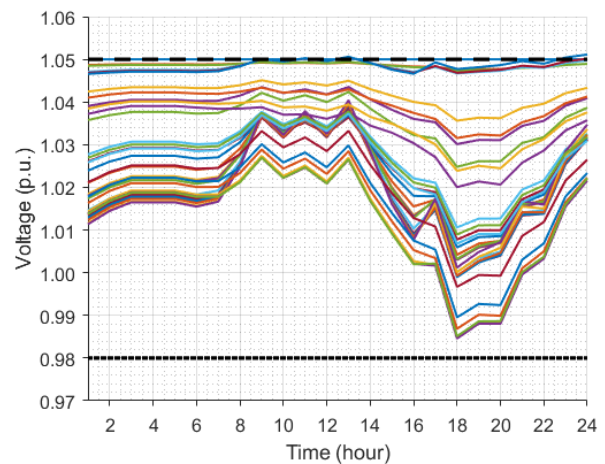
FIGURE 11. The 24h voltage profile of all buses with voltage scheme control considering BESS.

FIGURE 9. General Configuration of case study on 33-bus system.

Fig 11 shows the 24-hour voltage profiles after applying the coordinated control policies using the PJ-ADMM algorithm. In this case, excess active power injection from the PV inverters is absorbed by the grid and stored in storage to mitigate the voltage rise problem during 10:00-15:00. When all bus voltages are in the secure range, BESS systems do not provide further support. The results show that the proposed technique significantly improves voltage. As seen, allocating the BESS helps maximize the discharging mode's benefits, providing peak shaving and load control in the system.
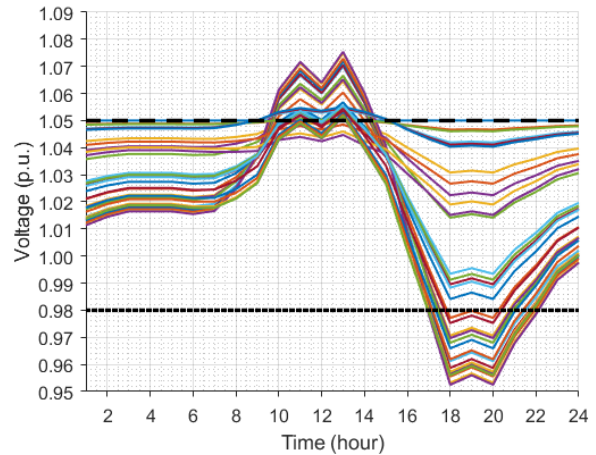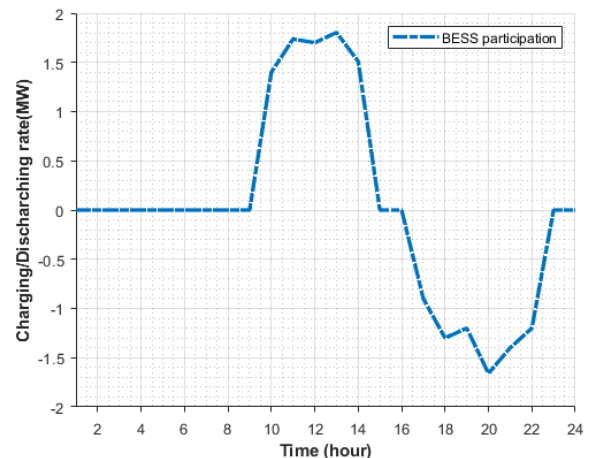

FIGURE 12. BESS participation.

The total charge and discharge rates for each hour of the day for four BESSs are shown in Fig. 12. The BESS is

charged during high PV generation and discharged during on-peak load periods. Note that in the cycle of the optimization algorithm, the power is proportionally shared between the BESS according to their capacity and load demand at each hour. The figure illustrates that the BESSs are charged during high PV generation and discharged during high load demand periods, and BESS's charge and discharge efficiencies were set to 95%. For the peak hour of the day, at 13:00, approximately 1.8 MW losses of active power were reduced by charging four BESSs, which is almost the same as the maximum discharging rate at 20:00. The results presented in Fig. 12 validate the effectiveness of the proposed mathematical optimisation method under peak-shaving or load-levelling scenarios.

G. 141-BUS SYSTEM

The proposed voltage control model has been thoroughly tested on both small-scale and large-scale systems, showcasing its versatility and scalability. In the case study, the system was expanded from a 33-bus network (comprised of 20 PV smart inverters and 4 BESSs) to a 141-bus network (comprised of 35 PV smart inverters and 3 BESSs), and the capacity of the PV panels was increased from 0.2 MW to 0.7 MW. The results from the case study on the 141-bus system, which was conducted using the same PV generation and load data as previous case studies, highlight the scalability of the proposed method. It was ensured that each bus maintained a secure voltage within the range of [0.95, 1.05] p.u. and that the PV panels were capable of operating at a power factor of up to 0.9.

As shown in Fig 13, without the proposed distributed voltage control strategy, the voltage profiles of the 141-bus system exceeded the maximum voltage limit between 10:00 and 14:00. Over-voltage (1.07 p.u.) was observed at midday, while some buses experienced under-voltage (0.92 p.u.) during the evening. With the proposed voltage control scheme, the system operator can effectively address the issue of rising
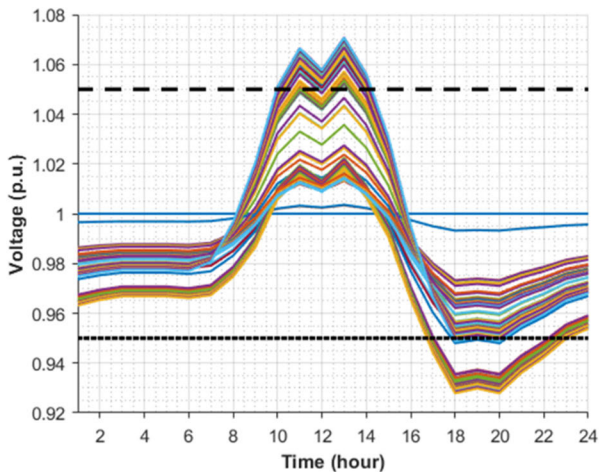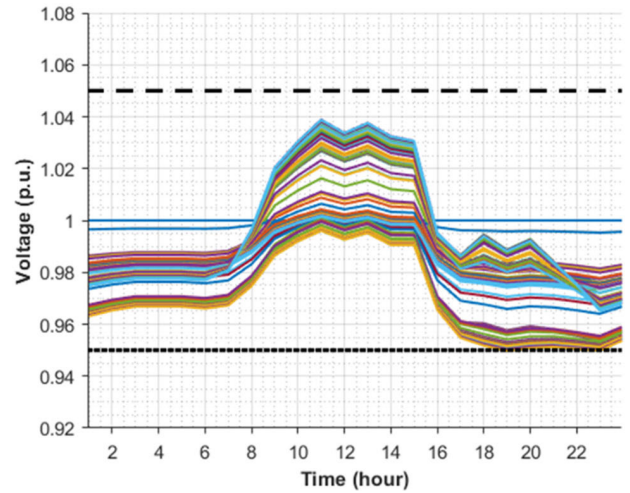

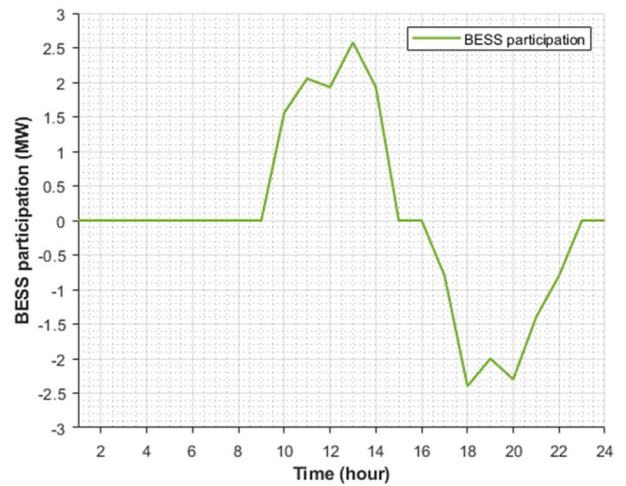**FIGURE 14.** The 24h voltage profile of 141-bus network with PV-BES voltage control.

FIGURE 15. Charging discharging rate (MW) for each BESS in 141-bus system.

voltage through the voltage regulation process. As illustrated in Fig 14, after applying the coordinated voltage control policy using the PJ-ADMM algorithm, a significant improvement in the voltage profile was achieved, demonstrating the scalability of the proposed method. The figure shows 24-hour profiles of bus voltages in the 141-bus system and it can be seen that when voltages increase more than 1.05 p.u, the BESS will start to charge and absorb the active power from the grid.

The results of the case studies demonstrate that the proposed method is both robust and scalable, making it a viable solution for voltage control in large-scale PV-integrated power systems. The BESS starts to discharge power to the grid when voltages drop below 0.95 p.u. When all bus voltage levels are stabilized within normal limits, there is no longer a need to make changes to the active power output of the BESSs. This study aimed to examine the potential reduction in power loss in power systems with high PV penetration and

FIGURE 13. Voltage profiles of 141-bus system with no voltage control.

S. R. Far et al.: ADMM-Based Multi-Objective Control Scheme for Mitigating the Impact of High Penetration DER Integration

IEEE Access

TABLE 6. Power loss reduction with BESs.

Number of PV in the system	Power Generation (MW)	BESS capacity (MWh)
35	21	2.5
38	23	3.4

to highlight the role of storage systems in mitigating these losses. To that end, we calculated the maximum reduction in power loss at midday and found that the use of virtual BESS with the PJ-ADMM algorithm resulted in a reduction of approximately 2.5MW per BESS, or up to 10 MWh in daily energy losses.

It was observed that power loss increased during charging hours and decreased during discharging hours. The optimal time to discharge BESSs was found to be during peak hours when electricity demand spikes, leading to an increase in active power loss. Fig 15 displays the participation rate of BESSs and provides a visual representation of their charge and discharge in MW over a 24-hour period. The figure shows that the PJ-ADMM algorithm evenly distributes power based on each BESS's capacity, with each BESS charging approximately 2.5 MW at 13:00 and reaching a total charging power of 7.7 MW for all three BESSs, which represents the discharged energy amount at hour 18. This study highlights the importance of incorporating storage systems, such as BESS, into power systems with high PV penetration to reduce energy loss and improve overall system performance.

Table 6 presents a clear correlation between the rise in PV power generation and the increased capacity of BESS. The data demonstrates that for every 10% increase in PV generation at 13:00, there is approximately a 30% increase in BESS capacity. This strong positive relationship between rising PV power generation and BESS capacity emphasizes the significance of incorporating BESS into renewable energy systems to enhance their overall efficiency and performance. For example, the data shows that with the installation of 38 PV units and a 3.4 MWh BESS capacity, there is a 30% increase in BESS capacity compared to the case of 35 PV installations. This highlights the benefits of incorporating BESS into renewable energy systems to effectively manage and store excess energy generated by PV units.

Fig. 16 provides a visual representation of the voltage convergence performance at node 29 at 13:00 for a smart inverter. To assess the impact of network size on the performance of the control algorithm, a comparison was made between the 33-bus and 141-bus networks. The results in the 141-bus network indicated that the PJ-ADMM algorithm with BESS converged to the optimal solution relatively quickly, reaching it after approximately 14 iterations. In contrast, the 33-bus network required only 10 iterations to reach the optimal solution. Each iteration of the JP-ADMM control took about 3 seconds, and the case studies revealed that the JP-ADMM took approximately 0.5 minutes (10 iterations) in the
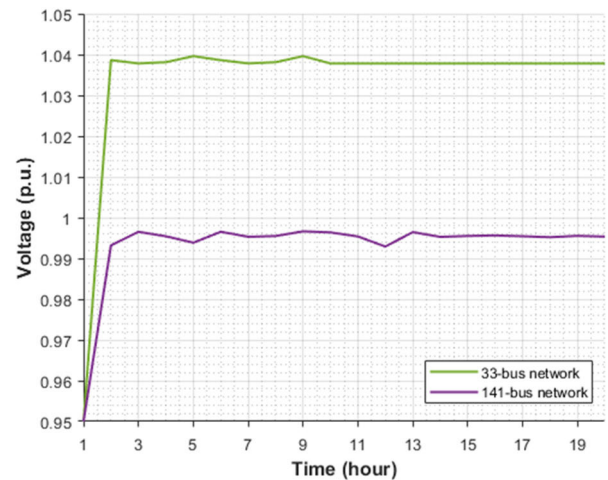
FIGURE 16. Voltage convergence at node 29 at 13:00.
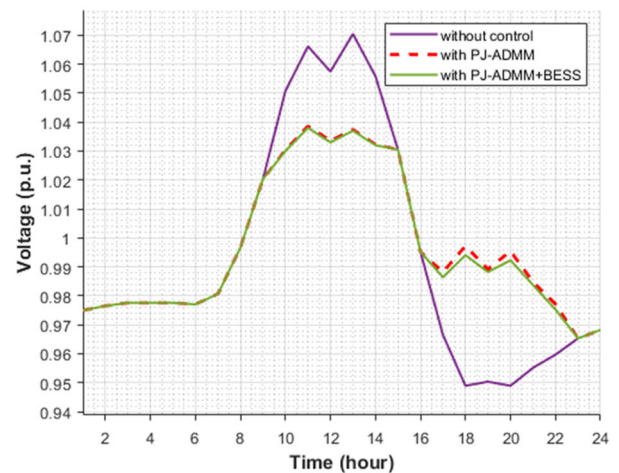
FIGURE 17. Voltage profile with and without control compared with BESS at node 28.

33-bus network and 0.75 minutes (14 iterations) in the 141-bus network to converge voltage at each bus to its limits. Although the increase in the system's size and the corresponding increase in the number of iterations led to an increase in calculation time, the JP-ADMM method still maintained a reasonable convergence rate. This highlights the effectiveness and importance of this method, as the increase in the number of agents was not proportional to the increase in the number of iterations required for convergence.

The proposed voltage control model was rigorously evaluated to determine its effectiveness. To do this, a comparison was made between the results obtained from the proposed model and those obtained from the default profile without control at node 28. The results of the comparison were visualized in Fig 17 and provided conclusive evidence of the success of the proposed model in reducing energy losses. The results showed that regulating voltage, either through a distributed control approach or using BESSs, produced the same optimal solution during over voltage periods. However,

IEEE *Access*

S. R. Far et al.: ADMM-Based Multi-Objective Control Scheme for Mitigating the Impact of High Penetration DER Integration

during under voltage periods, the proposed coordinated voltage control model was found to be superior to the original algorithm and default profile without control. This highlights the versatility and effectiveness of the proposed model in achieving the desired outcome of stable and efficient voltage regulation, which effectively reduces energy losses and provides the same optimal solution in voltage regulation.

VI. CONCLUSION

In this study, a fully distributed control scheme for smart PV inverters based on the PJ-ADMM algorithm was proposed for reducing power loss by determining charging/discharging control actions for BESSs. A new approach of incorporating virtual BESSs into the PJ-ADMM algorithm for voltage control was introduced, allowing network operators to utilize storage systems without active power curtailment. The proposed method demonstrated the capability of smart inverters to handle uncertainty associated with PV systems and provide voltage support through either active or reactive power. The optimal utilization of PV power was ensured by locally controlling smart PV inverters through the PJ-ADMM algorithm in cooperation with BESSs, with charging/discharging rates allocated based on minimum curtailment. The scalability of the method was demonstrated with the 141-bus distribution feeder, showing that voltage rise/drop issues were mitigated at midday and evening through the use of installed BESSs. Simulation results validated that the strategy could maintain voltage profiles within established constraints and minimize PV power loss, highlighting the effectiveness and robustness of the control scheme. The voltage profiles of the 141-bus system without the proposed distributed voltage control strategy exceeded the upper voltage and under voltage limits with 1.07 p.u. at 13:00 and 0.92 p.u. at 20:00, respectively. Applying the coordinated voltage control policy demonstrates a significant improvement which validates the scalability of the proposed method The results of the simulation show 10 MWh reduction in daily energy losses is possible using virtual BESS for the PJ-ADMM algorithm. Future research can be conducted in several areas. One possibility is to investigate how the proposed method can be extended to create a scalable platform that includes various renewable energy sources, energy storage systems, and electric vehicles that can communicate with each other through a powerful control system. Additionally, developing an intelligent method for training agents using neural networks that aims to reduce the running time of distributed algorithms and investigating the impact of reactive power regulations on the frequency control of the system could also be beneficial.

REFERENCES

[1] T. Tewari, A. Mohapatra, and S. Anand, "Coordinated control of OLTC and energy storage for voltage regulation in distribution network with high PV penetration," *IEEE Trans. Sustain. Energy*, vol. 12, no. 1, pp. 262–272, Jan. 2021.

[2] T. Zhao and Z. Ding, "Distributed agent consensus-based optimal resource management for microgrids," *IEEE Trans. Sustain. Energy*, vol. 9, no. 1, pp. 443–452, Jan. 2018.

[3] P. Li, M. Yang, Y. Tang, Y. Yu, and M. Li, "Robust decentralized coordination of transmission and active distribution networks," *IEEE Trans. Ind. Appl.*, vol. 57, no. 3, pp. 1987–1994, May/Jun. 2021.

[4] X. Wang, "Optimal voltage regulation for distribution networks with multi-microgrids," *Appl. Energy*, vol. 210, pp. 1027–1036, Jan. 2018.

[5] N. Mahmud and A. Zahedi, "Review of control strategies for voltage regulation of the smart distribution network with high penetration of renewable distributed generation," *Renew. Sustain. Energy Rev.*, vol. 64, pp. 582–595, Oct. 2016.

[6] A. Safavizadeh, G. R. Yousefi, and H. R. Karshenas, "Voltage variation mitigation using reactive power management of distributed energy resources in a smart distribution system," *IEEE Trans. Smart Grid*, vol. 10, no. 2, pp. 1907–1915, Mar. 2019.

[7] Y. Zhang, K. Meng, F. Luo, H. Yang, J. Zhu, and Z. Y. Dong, "Multi-agent-based voltage regulation scheme for high photovoltaic penetrated active distribution networks using battery energy storage systems," *IEEE Access*, vol. 8, pp. 7323–7333, 2020.

[8] T. Xu and W. Wu, "Accelerated ADMM-based fully distributed inverter-based Volt/Var control strategy for active distribution networks," *IEEE Trans. Ind. Informat.*, vol. 16, no. 12, pp. 7532–7543, Dec. 2020.

[9] T. Gush, C.-H. Kim, S. Admasie, J.-S. Kim, and J.-S. Song, "Optimal smart inverter control for PV and BESS to improve PV hosting capacity of distribution networks using slime mould algorithm," *IEEE Access*, vol. 9, pp. 52164–52176, 2021.

[10] M. Zeraati, M. E. H. Golshan, and J. M. Guerrero, "Distributed control of battery energy storage systems for voltage regulation in distribution networks with high PV penetration," *IEEE Trans. Smart Grid*, vol. 9, no. 4, pp. 3582–3593, Jul. 2018.

[11] M. Mohammadjafari, R. Ebrahimi, and V. Parvin Darabad, "Optimal energy management of a microgrid incorporating a novel efficient demand response and battery storage system," *J. Electr. Eng. Technol.*, vol. 15, no. 2, pp. 571–590, Mar. 2020.

[12] J. Lopez-Lorente, X. A. Liu, R. J. Best, G. Makrides, and D. J. Morrow, "Techno-economic assessment of grid-level battery energy storage supporting distributed photovoltaic power," *IEEE Access*, vol. 9, pp. 146256–146280, 2021.

[13] K. E. Antoniadou-Plytaria, I. N. Kouveliotis-Lysikatos, P. S. Georgilakis, and N. D. Hatziargyriou, "Distributed and decentralized voltage control of smart distribution networks: Models, methods, and future research," *IEEE Trans. Smart Grid*, vol. 8, no. 6, pp. 2999–3008, Nov. 2017.

[14] Y. Z. Gerdroodbari, R. Razzaghi, and F. Shahnia, "Decentralized control strategy to improve fairness in active power curtailment of PV inverters in low-voltage distribution networks," *IEEE Trans. Sustain. Energy*, vol. 12, no. 4, pp. 2282–2292, Oct. 2021.

[15] L. Wang, D. H. Liang, A. F. Crossland, P. C. Taylor, D. Jones, and N. S. Wade, "Coordination of multiple energy storage units in a low-voltage distribution network," *IEEE Trans. Smart Grid*, vol. 6, no. 6, pp. 2906–2918, Nov. 2015.

[16] M. Bahramipanah, R. Cherkaoui, and M. Paolone, "Decentralized voltage control of clustered active distribution network by means of energy storage systems," *Electr. Power Syst. Res.*, vol. 136, pp. 370–382, Jul. 2016.

[17] M. Bazrafshan and N. Gatsis, "Decentralized stochastic optimal power flow in radial networks with distributed generation," *IEEE Trans. Smart Grid*, vol. 8, no. 2, pp. 787–801, Mar. 2017.

[18] J. von Appen, T. Stetz, M. Braun, and A. Schmiegel, "Local voltage control strategies for PV storage systems in distribution grids," *IEEE Trans. Smart Grid*, vol. 5, no. 2, pp. 1002–1009, Mar. 2014.

[19] N. Nikmehr, "Distributed robust operational optimization of networked microgrids embedded interconnected energy hubs," *Energy*, vol. 199, May 2020, Art. no. 117440.

[20] Y. Liu, L. Guo, C. Lu, Y. Chai, S. Gao, and B. Xu, "A fully distributed voltage optimization method for distribution networks considering integer constraints of step voltage regulators," *IEEE Access*, vol. 7, pp. 60055–60066, 2019.

[21] A. Rajaei, S. Fattaheian-Dehkordi, M. Fotuhi-Firuzabad, M. Moeini-Aghtaie, and M. Lehtonen, "Developing a distributed robust energy management framework for active distribution systems," *IEEE Trans. Sustain. Energy*, vol. 12, no. 4, pp. 1891–1902, Oct. 2021.

[22] M. Wang, Y. Su, L. Chen, Z. Li, and S. Mei, "Distributed optimal power flow of DC microgrids: A penalty based ADMM approach," *CSEE J. Power Energy Syst.*, vol. 7, no. 2, pp. 339–347, Mar. 2021.

S. R. Far et al.: ADMM-Based Multi-Objective Control Scheme for Mitigating the Impact of High Penetration DER Integration

IEEE Access

[23] Y. Liu, "Distributed robust energy management of a multi-microgrid system in the real-time energy market," *IEEE Trans. Sustain. Energy*, vol. 10, no. 1, pp. 396–406, Jan. 2019.

[24] G. Chen and Q. Yang, "An ADMM-based distributed algorithm for economic dispatch in islanded microgrids," *IEEE Trans. Ind. Informat.*, vol. 14, no. 9, pp. 3892–3903, Sep. 2018.

[25] W. Zheng, W. Wu, B. Zhang, H. Sun, and Y. Liu, "A fully distributed reactive power optimization and control method for active distribution networks," *IEEE Trans. Smart Grid*, vol. 7, no. 2, pp. 1021–1033, Mar. 2016.

[26] A. Kargarian, J. Mohammadi, J. Guo, S. Chakrabarti, M. Barati, G. Hug, S. Kar, and R. Baldick, "Toward distributed/decentralized DC optimal power flow implementation in future electric power systems," *IEEE Trans. Smart Grid*, vol. 9, no. 4, pp. 2574–2594, Jul. 2018.

[27] S. Huang, Q. Wu, Y. Guo, X. Chen, B. Zhou, and C. Li, "Distributed voltage control based on ADMM for large-scale wind farm cluster connected to VSC-HVDC," *IEEE Trans. Sustain. Energy*, vol. 11, no. 2, pp. 584–594, Apr. 2020.

[28] S. Magnússon, P. C. Weeraddana, and C. Fischione, "A distributed approach for the optimal power-flow problem based on ADMM and sequential convex approximations," *IEEE Trans. Control Netw. Syst.*, vol. 2, no. 3, pp. 238–253, Sep. 2015.

[29] H. J. Liu, W. Shi, and H. Zhu, "Distributed voltage control in distribution networks: Online and robust implementations," *IEEE Trans. Smart Grid*, vol. 9, no. 6, pp. 6106–6117, Nov. 2018.

[30] W. Ananduta, C. Ocampo-Martinez, and A. Nedic, "A distributed augmented Lagrangian method over stochastic networks for economic dispatch of large-scale energy systems," *IEEE Trans. Sustain. Energy*, vol. 12, no. 4, pp. 1927–1934, Oct. 2021.

[31] H. Almasalma, S. Claeys, and G. Deconinck, "Peer-to-peer-based integrated grid voltage support function for smart photovoltaic inverters," *Appl. Energy*, vol. 239, pp. 1037–1048, Apr. 2019.

[32] S. D. Manshadi, G. Liu, M. E. Khodayar, J. Wang, and R. Dai, "A distributed convex relaxation approach to solve the power flow problem," *IEEE Syst. J.*, vol. 14, no. 1, pp. 803–812, Mar. 2020, doi: 10.1109/JSYST.2019.2913133.

[33] W. Deng, M. Lai, Z. Peng, and W. Yin, "Parallel multi-block ADMM with O(1/K) convergence," UCLA, Los Angeles, CA, USA, Tech. Rep. CAM 13-64, 2013.

[34] P. Olivella-Rosell, F. Rullan, P. Lloret-Gallego, E. Prieto-Araujo, R. Ferrer-San-Jose, S. Barja-Martinez, S. Bjarghov, V. Lakshmanan, A. Hentunen, J. Forsstrom, S. O. Ottesen, R. Villafafila-Robles, and A. Sumper, "Centralised and distributed optimization for aggregated flexibility services provision," *IEEE Trans. Smart Grid*, vol. 11, no. 4, pp. 3257–3269, Jul. 2020, doi: 10.1109/TSG.2019.2962269.

[35] M. Li, J. Gao, N. Chen, L. Zhao, and X. Shen, "Decentralized PEV power allocation with power distribution and transportation constraints," *IEEE J. Sel. Areas Commun.*, vol. 38, no. 1, pp. 229–243, Jan. 2020, doi: 10.1109/JSAC.2019.2951989.

[36] Y. Guo, Q. Wu, H. Gao, S. Huang, B. Zhou, and C. Li, "Double-time-scale coordinated voltage control in active distribution networks based on MPC," *IEEE Trans. Sustain. Energy*, vol. 11, no. 1, pp. 294–303, Jan. 2020.

[37] X. Kou, F. Li, J. Dong, M. Starke, J. Munk, Y. Xue, M. Olama, and H. Zandi, "A scalable and distributed algorithm for managing residential demand response programs using alternating direction method of multipliers (ADMM)," *IEEE Trans. Smart Grid*, vol. 11, no. 6, pp. 4871–4882, Nov. 2020.

[38] W. Li, Y. Liu, H. Liang, and Y. Shen, "A new distributed energy management strategy for smart grid with stochastic wind power," *IEEE Trans. Ind. Electron.*, vol. 68, no. 2, pp. 1311–1321, Feb. 2021.

[39] H. Almasalma and G. Deconinck, "Robust policy-based distributed voltage control provided by PV-battery inverters," *IEEE Access*, vol. 8, pp. 124939–124948, 2020.

[40] L.-Y. Lu and C.-C. Chu, "Consensus-based droop control of isolated micro-grids by ADMM implementations," in *Proc. IEEE Power Energy Soc. Gen. Meeting (PESGM)*, Aug. 2018, p. 1.

[41] J. Lofberg, "YALMIP: A toolbox for modeling and optimization in MATLAB," in *Proc. IEEE Int. Conf. Robot. Autom.*, Oct. 2004, pp. 284–289.

[42] R. D. Zimmerman and C. E. Murillo-Sanchez. (2019). *MATPOWER (Version 7.0)*. [Online]. Available: https://matpower.org/

[43] *Additional Document Review*, Online Document, Dropbox, San Francisco, CA, USA, Oct. 2021. [Online]. Available: https://www.dropbox.com/s/v5ivvaipyijms0g/additional_document_review.pdf

SADAF RAHIMI FAR (Graduate Student Member, IEEE) received the M.Sc. degree in electrical and electronics engineering from Coventry University, Coventry, England, U.K., in 2017. She is currently pursuing the Ph.D. degree in electrical engineering with École de Technologie Supérieure (ÉTS), Université du Québec, Montréal, QC, Canada. Her current research interests include optimization control, distributed power generation, photovoltaic systems, power system voltage control, and battery energy storage.

ALI MOEINI (Senior Member, IEEE) received the Ph.D. degree in electrical engineering from Laval University, Quebec City, QC, Canada, in 2016. In 2014, he joined Hydro-Québec Research Institute (IREQ), Varennes, QC, Canada. His main research interests include integrated power system planning, operation, and control, distributed energy resources, smart grids, smart cities, and optimization methods.
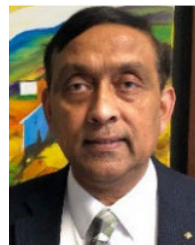
AMBRISH CHANDRA (Fellow, IEEE) received the B.E. degree from the University of Roorkee (currently IITR), India, in 1977, the M.Tech. degree from IIT Delhi, in 1980, and the Ph.D. degree from the University of Calgary, in 1987. Before joining as an Associate Professor with École de Technologie Supérieure (ÉTS), Montréal, in 1994, he was an Associate Professor with IITR. Since 1999, he has been a Full Professor of electrical engineering with ÉTS. From 2012 to 2015, he was the Director of the Multidisciplinary Graduate Program on Renewable Energy and Energy Efficiency, ÉTS, where he is currently the Director of the master's program in electrical engineering. He is the coauthor of the book *Power Quality: Problems and Mitigation Techniques* (Wiley). His research interests include the advancement of new theory and control algorithms for power electronic converters for power quality improvement in distribution systems and the integration of renewable energy sources. He is a fellow of many organizations, including the Canadian Academy of Engineering; the Institute of Engineering and Technology, U.K.; and the Engineering Institute of Canada. He was a recipient of the IEEE Canada P. Ziogas Electric Power Award 2018 and the IEEE Power and Energy Society Nari Hingorani Custom Power Award 2021. He is registered as a Professional Engineer in Quebec.

INNOCENT KAMWA (Fellow, IEEE) received the Ph.D. degree in electrical engineering from Laval University, in 1989. He is currently a Full Professor with the Department of Electrical Engineering and the Tier 1 Canada Research Chair in decentralized sustainable electricity grids for smart communities with Laval University. Previously, he was a Researcher with Hydro-Québec Research Institute, specializing in the dynamic performance and control of power systems. He was also the Chief Scientist of the Hydro-Québec Smart Grid Innovation Program and an international consultant in power grid simulation and network stability. He is a fellow of the Canadian Academy of Engineering and the IEEE for his innovations in power system control. He was a recipient of the 2019 IEEE Charles Proteus Steinmetz Award and the Charles Concordia Award. He was the Editor-in-Chief of the *IET Generation, Transmission, and Distribution*. He is currently the Editor-in-Chief of *IEEE Power and Energy Magazine* and an Associate Editor of IEEE Transactions on Power Systems.

● ● ●